CircINSR regulates fetal bovine muscle and fat development

Xuemei Shen
Northwest Agriculture and Forestry University https://orcid.org/0000-0003-3451-0204
Jia Tang
Northwest Agriculture and Forestry University
Wenxiu Ru
Northwest Agriculture and Forestry University
Xiaoyan Zhang
Northwest Agriculture and Forestry University
Yongzhen Huang
Northwest Agriculture and Forestry University
Xianyong Lan
Northwest Agriculture and Forestry University
Chuzhao Lei
Northwest Agriculture and Forestry University
Hui Cao
Shaanxi Province
Hong Chen (chenhong1212@263.net)
Northwest Agriculture and Forestry University

Methodology article

Keywords: Bovine, Muscle development, Circular RNAs, Cell proliferation, Preadipocyte

Posted Date: September 21st, 2020

DOI: https://doi.org/10.21203/rs.3.rs-79997/v1

Abstract

Background: The level of muscle development directly affects the production efficiency of livestock, and the content of intramuscular fat (IMF) is an important factor affecting meat quality. Nevertheless, the molecular mechanism of embryonic circular RNA in muscle and IMF development remains largely unknown.

Methods: In this study, we isolated myoblasts and intramuscular preadipocytes from fetal bovine skeletal muscle. Oil Red O and BODIPY staining were used to identify lipid droplets of preadipocytes, and anti-MyHC immunofluorescence was used to identify myotubes differentiated from myoblasts. Bioinformatics, dual fluorescence reporter system, and RNA immunoprecipitation were used to determine the interactions between circINSR and miR-15/16 family. Molecular and biochemical assays were used to confirm the role of circINSR in myoblasts and intramuscular preadipocytes.

Results: We found that the isolated myoblasts and preadipocytes can differentiate normally. Besides, circINSR severed as a sponge of miR-15/16 family, which targeting *CyclinD1* and *Bcl-2*. CircINSR overexpression significantly promoted myoblasts and preadipocytes proliferation, and inhibited cell apoptosis. In addition, circINSR inhibited preadipocytes adipogenesis by alleviating the inhibition of miR-15/16 on target genes *FOXO1* and *EPT1*.

Conclusions: Taken together, our study demonstrated circINSR as a regulator of embryonic muscle and IMF development.

1. Introduction

In livestock production, the development of muscle and intramuscular fat (IMF) is an important factor in ensuring meat quality. Bovine muscle development begins in the early embryonic stage, including the proliferation of myoblast progenitor cells, as well as the proliferation and fusion of mononuclear myoblasts form multinucleated myotubes. After birth, the number of muscle fibers will not change, but the fibers become thicker(1, 2). Therefore, the level of muscle development during pregnancy directly affects the meat production. Fat starts to develop in the second trimester(3). The content of the IMF is related to the tenderness and juiciness of beef, which has always been a research hotspot. Increasing the number of preadipocytes in the fetal muscle helps to deposit fat and marbling after birth(4). However, the mechanism of muscle and IMF development is still unclear. In addition, premature adipogenesis and maturation of intramuscular preadipocytes in the fetus may cause muscle tissue dysfunction(5). Therefore, it is of great significance to explore the molecular mechanism of muscle and IMF development.

The development of biotechnology has greatly promoted the screening and research of key genes for muscle and IMF development. Several critical genes have been demonstrated to mediate muscle development and adipogenesis. For instance, peroxisome proliferative activated receptor (*PPARγ*) and CCAAT/enhancer binding protein (*C/EBPα*) have been characterized as the regulators of adipogenesis(6,

7). The myogenic regulatory factors (*MRFs*), myocyte enhancer factor (*MEF*2), *PAX3/PAX7*, and myostatin (*MSTN*) have been reported to be effective in inducing myoblasts proliferation and differentiation(8-12).

In addition to coding genes, a large number of non-coding RNAs have also been proven to regulate muscle and fat development. For example, a large number of miRNAs and circRNAs have been reported to participate in the physiological regulation of muscle and fat. CircRNAs have a covalent closed loop structure, neither 5'-3' polarity nor polyadenylated tail(13). They can participate in physiological regulation by sponging miRNAs or binding regulatory proteins(14). In existing reports, circFUT10 and circFGFR4 regulate the muscle development related genes through sponge miR-133a and miR-107(15, 16). CircINSR adsorb miR-34a to promote the proliferation of bovine myoblasts(17). CircTshz2-1 and circArhgap5-2 have been shown to be indispensable regulators of fat formation(18). Despite these findings, the role of circRNAs in muscle and IMF development still requires further research.

In this study, we isolated fetal bovine myoblasts and intramuscular preadipocytes. The targeting relationship between circINSR and miR-15/16 family and the effect of circINSR on the proliferation and apoptosis of myoblasts and preadipocytes were analyzed in vitro. Importantly, we proved that circINSR can target miR-15/16 to inhibit the premature differentiation of intramuscular preadipocytes, thereby ensuring the normal of muscle function.

2. Materials And Methods

2.1 Progenitor cells isolation and cell lines.

Bovine fetuses for 120~180 days were collected from the slaughterhouse and transported to the laboratory immediately. Using the enzyme digestion combined with the differential adhesion method, the primary myoblasts and intramuscular preadipocytes were isolated from the longissimus dorsi as previously described (19). The longissimus dorsi was isolated from the fetus, washed with phosphate buffered saline (PBS), and minced into small fragments. It was then digested in Dulbecco's modified Eagle's medium (DMEM) containing type IV collagenase (w/v, 0.2%; C5138, Sigma, USA) at 37°C with continuous shaking for 2 hours. The cell plasma was filtered through the 200 μm filter, collected by centrifugation and resuspended in DMEM. The cells were seeded in complete medium and incubated at 37 °C with 5% CO_2. The adherent cells within two hours of inoculation were collected for adipogenesis induction. After 24 hours of culture, the non-adherent cell suspension was re-inoculated. After repeated operations for 2 days, adherent cells were collected for myogenesis induction. HEK-293T cells were purchased from the American Type Culture Collection (ATCC) and were tested negative for mycoplasma contamination.

2.2 Differentiation of myoblasts and preadipocytes.

Myoblasts were cultured in high-glucose DMEM supplemented with 20% fetal bovine serum (FBS, Gibco). 2 days after cells reached confluence, DMEM containing 2% horse serum was used for myogenesis

induction. Myotube identification was performed on the 4th day of induction. Intramuscular preadipocytes were cultured in F12/DMEM supplemented with 10% FBS. Adipocyte differentiation was induced by M1 medium (containing 0.5 mM 3-isobutyl-1-methylxanthine, 1 μM dexamethasone, and 1.5 μg/mL insulin). 2 days later, the M1 medium was replaced with M2 medium (containing 1.5 μg/mL insulin). Then differentiation was induced for 8 days, during which the medium was changed once every 2 days. The M2 medium was changed every two days, and Oil Red O staining was performed on the 8th day of adipogenic differentiation.

2.3 RNA extraction and real-time qPCR

Total RNA was isolated with Trizol reagent (Invitrogen, Carlsbad, CA, USA) and cDNA was synthesized with PrimeScript™ RT reagent kit with gDNA Eraser (Takara, Tokyo, Japan). Real-time qPCR for RNA analyses were performed using SYBR Green PCR Master Mix (Takara, Tokyo, Japan). MiRNAs specific stem-loop primers were used for reverse transcription. The level of GAPDH was used to normalize the expression of circRNA and mRNA, and the level of small nuclear U6 was used to normalize the expression levels of miRNAs.

2.4 Vector construction and cell transfection

The second exon sequence of *INSR* gene was constructed into pCD2.1 vector and psi-CHECK2 vector. Small interfering RNA (siRNA) oligonucleotides were designed to combine with the back-splice region of circINSR (RiboBio, Guangzhou, China). The mimics of bta-miR-15a, bta-miR-15b, bta-miR-16a, and bta-miR-16b were purchased from RiboBio (Guangzhou, China). The 3'-UTRs of *CCND*1 and *Bcl*-2 genes containing the miR-15/16 binding sites were amplified by PCR enzyme mix (Platinum II Taq Hot-Start DNA Polymerase, Invitrogen). The wild-type and mutant 3'-UTR gene sequences were cloned into the psi-CHECK2 vector. The mimics (50 nM) or vectors (2 μg/mL) were transfected into cells with transfection reagent (R0531, Thermo Fisher Scientific, USA). For overexpression of miR-15/16 family, a quarter of miR-15a, miR-15b, miR-16a, and miR-16b mimics were selected and mixed in equal amounts for transfection.

2.5 Oil Red O and BODIPY staining

After 8 days of differentiation, the intramuscular preadipocytes were stained with Oil red O (O0625, sigma, USA) and 4,4-difluoro-1,3,5,7,8-pentamethyl-4-bora-3a,4a-diaza-s-indacene (BODIPY 493/503) (D3922, Thermo Fisher Scientific). Oil Red O dyeing was performed according to the instructions. To quantify staining in fat droplets, the 100% isopropanol was used to dissolve the lipid droplets, and measure the absorbance at 510 nm. For BODIPY staining, the cells were washed twice with PBS to remove residual 4% paraformaldehyde. Hank's Balanced Salt Solution with 10 μM BODIPY 493/503 was added to the cells and then incubated at 37°C for 30 minutes in the dark. The samples were washed 3 times with PBS and photographed immediately.

2.6 Immunofluorescence analysis

After 4 days of myogenic differentiation, the myoblasts were fixed with 4% paraformaldehyde. After washing with PBS, MyHC antibody (1:250, Heavy chain cardiac Myosin antibody, GTX20015, GeneTex, USA) was added to incubate overnight at 4°C, and then the secondary antibody was added to incubate for 2 hours. The nucleus was stained with DAPI. The myotube coverage area was analyzed by Image pro plus software.

2.7 Dual Luciferase Reporter Assay

HEK-293T cells were co-transfected with miR-15/16 mimics and plasmid. After 24 hours of transfection, the luciferase activity was detected with the Dual-Luciferase Reporter Assay Kit (E2920, Promega, Fitchburg, WI, USA). The optical density of the resulting solution was assessed using the automatic microplate reader (Molecular Devices, Sunnyvale, USA).

2.8 RNA-binding protein immunoprecipitation (RIP)

RNA-binding protein immunoprecipitation assay was performed using EZ-Magna RIP kit (17-701, Millipore, Billerica, MA, USA) according to the manufacturer's instructions. The Argonaute2 (Ago2) antibody (Abcam, UK) and IgG antibody were used for immunoprecipitation. The RNA was extracted from the immunoprecipitation products of myoblasts and preadipocytes, and the abundance of circINSR and miR-15/16 was detected by real-time qPCR.

2.9 5-Ethynyl-2`-deoxyuridine (EdU) and Cell Counting Kit-8 (CCK-8) assay

When the density of myoblasts and preadipocytes reached 40%-50%, the transfection was performed with overexpression plasmid, siRNA or miRNA mimics. After 24 hours of transfection, the cell proliferation was tested by EdU assay kit (RiboBio, Guangzhou, China). The nucleus was stained with Hoechst 33342. Use a fluorescence microscope to take pictures immediately after staining (AMG EVOS, Seattle, WA, USA). Similarly, we also used the CCK-8 (Multisciences, Hangzhou, China) to detect the level of cell proliferation after transfection. The optical density of CCK-8 at 450 nm was measured using an automatic microplate reader (Synergy4, BioTek, Winooski, USA).

2.10 Cell cycle and apoptosis assay

We used flow cytometry and the Cell Cycle Testing Kit (Multisciences, Hangzhou, China) to analyze the cell cycle. The myoblasts and preadipocytes were transfected when the cell growth density reached 50%. After transfection for 24 hours the cells were collected and washed with PBS. Subsequently, follow the kit instructions for staining. Flow cytometry analysis was performed on a BD Accuri C6 flow cytometer (BD Biosciences, USA). Cell apoptosis assays were performed with Annexin V-PE/7-AAD Apoptosis Detection Kit (RiboBio, Guangzhou, China) according to the manufacturer's recommendations. Afterward, the apoptosis rate was analyzed using flow cytometry (FACS Canto™ II, BD BioSciences, USA).

2.11 Western Blot analysis

Proteins from cultured myoblasts and preadipocytes were lysed with RIPA buffer (Solarbio, Beijing, China). Proteins were loaded onto 12% SDS-PAGE gels and transferred to polyvinylidene difluoride (PVDF) membranes (Thermo Fisher Scientific). The membranes were incubated overnight with primary antibodies specific for anti-GAPDH (#ab9485), anti-CyclinD1 (#ab226977), (Abcam, Cambridge, UK), anti-Bcl-2 (#bs-0032R), anti-caspase-9 (#bs-0049R), anti-Bax (#bs-0127M), anti-FABP4 (#bsm-51247M) (Bioss, Beijing, China), anti-PCNA (#WL01804), anti-CDK2 (#WL01543), anti-PPARγ (#WL01800) and anti-C/EBPα (#WL01899) (Wanlei Bio, Shenyang, China) at 4℃. After incubation with secondary antibodies, the membranes were quantified with the chemiluminescence system (Bio Rad, Hercules, CA, USA).

2.12 Statistical analyses

Data are expressed as the mean ± standard error (SEM) of at least 3 independent experiments. Statistical analyses were performed using SPSS 19.0 statistical software (SPSS, Chicago, IL, USA). Statistically significant differences were calculated using Student`s *t*-test. A probability of 0.05 or less was considered statistically significant.

3. Results

3.1 Myoblasts and intramuscular preadipocytes were isolated from the bovine fetus.

Skeletal muscle and intramuscular adipose tissue differentiated from mesoderm mesenchymal stem cells (MSCs). Muscle begins to develop in the early embryonic period, and adipose tissue begins to occur in the second trimester(20) (Fig. 1A). Enzymatic digestion combined with differential adhesion method could roughly separate myoblasts and intramuscular preadipocytes. In this study, these isolated preadipocytes were spindle-shaped and possess the common characteristics of fibroblasts. After 8 days of adipogenic induction, small lipid droplets accumulated in some cells. The Oil Red O staining results also intuitively indicated that the isolated cells had undergone adipogenic differentiation (Fig. 1B). The results of BODIPY staining showed that 8 days of adipogenic induction caused lipid accumulation in intramuscular preadipocytes (Fig. 1C). In addition, the real-time qPCR results showed that the adipogenesis marker genes *PPARγ* and *C/EBPα* were significantly increased (Fig. 1E). At the same time, the results of MyHC immunofluorescence showed that the isolated myoblasts were also induced into some myotubes (Fig. 1D). And myogenic differentiation marker genes were also significantly overexpressed (Fig. 1F).

3.2 CircINSR serves as a sponge of miR-15/16.

Previous studies have shown that circINSR could adsorb miR-34a. In this study, after overexpression of circINSR in myoblasts and preadipocytes, real-time qPCR results showed that the expression of miR-15a, miR-15b, miR-16a, and miR-16b was significantly reduced (Fig. 2A, B). The binding sites for miR-15/16 family on circINSR were predicted using Target Scan 7.0 and miRanda (Fig. 2C). The results of the dual fluorescence reporter system showed that the overexpression of miR-15/16 family could significantly inhibit the activity of Renilla luciferase in the psi-CHECK2-circINSR vector (Fig. 2D). In order to verify this

adsorption, we performed Ago2-RIP assay in myoblasts and preadipocytes to detect the expression of endogenous circINSR and miR-15/16 bound to Ago2 protein. The results showed that the miR-15/16 family can be enriched by Ago2 protein in both myoblasts and preadipocytes (Fig. 2F, G). In Ago2 protein immunoprecipitation, the expression of circINSR was significantly higher than that of IgG group (Fig. 2E).

3.3 CircINSR promotes myoblasts proliferation and inhibits apoptosis.

Existing studies have reported that *CyclinD*1 and *Bcl-2* are the target genes of miR-15/16 family. We connected the wild type and mutant type of the 3'-UTR sequence containing the binding site into the psi-CHECK2 vector for verification of the dual fluorescent reporter gene system (Fig. 3A). The results showed that the overexpression of miR-15/16 family could significantly inhibit the activity of Renilla luciferase in the wild-type vector (Fig. 3B). *CyclinD1* gene is a key regulator of cell proliferation. Real-time qPCR results showed that the overexpression of miR-15/16 mixed mimics could significantly reduce the expression of *CyclinD*1 and other cell proliferation marker genes. However, co-transfection of circINSR and miR-15/16 could alleviate this inhibition (Fig. 3C). Further EdU results showed that the transfection of miR-15/16 mixed mimics could significantly reduce the number of proliferating cells, and co-transfection with circINSR could rescue this anti-proliferation effect (Fig. 3D, E). The CCK-8 cell proliferation analysis also obtained the same result (Fig. 3F). The cell cycle results showed that miR-15/16 blocked the cell cycle and reduced the number of cells entering the S phase, while co-transfection with circINSR alleviated this inhibition (Fig. 3G, H).

In order to verify the targeting relationship between miR-15/16 and *Bcl-2*, we constructed wild-type and mutant psi-CHECK2 vectors (Fig. 4A). The results of the fluorescence report analysis indicate that *Bcl-2* was a potential target gene of miR-15/16 (Fig. 4B). Real-time qPCR results showed that miR-15/16 significantly inhibited the expression of *Bcl-2* and promoted the expression of apoptosis marker genes *Bax* and *Caspase*9 (Fig. 4C). The subsequent flow cytometry analysis results showed that overexpression of miR-15/16 promoted myoblasts apoptosis, and co-transfection of circINSR reduced the number of apoptotic cells (Fig. 4D, E).

3.4 CircINSR promotes preadipocytes proliferation by sponging miR-15/16.

To investigate the role of circINSR in adipogenesis, preadipocytes were transfected with circINSR overexpression vector and siRNA. The results of real-time qPCR showed that overexpression of circINSR significantly promoted the expression of cell proliferation marker genes (Fig. 5A), while interference with circINSR inhibited the expression of these genes (Fig. 5B). The Western Blots showed the same results (Fig. 5C). In addition, transfection of mixed miR-15/16 mixed mimics in preadipocytes could significantly inhibit the expression of cell proliferation-related genes, while co-transfection with circINSR could restore this inhibition (Fig. 5D). The results of EdU (Fig. 5E, F) and CCK-8 (Fig. 5G) also showed that miR-15/16 inhibited cell proliferation, and co-transfection of miR-15/16 and circINSR alleviated this inhibition. Cell cycle assay showed that miR-15/16 inhibited preadipocytes entering S phase, and co-transfection with circINSR promoted cell proliferation (Fig. 5H, I).

3.5 CircINSR inhibits preadipocytes apoptosis by sponging miR-15/16.

To further explore the function of circINSR in preadipocytes apoptosis, real-time qPCR was used to detect the expression of apoptosis-related genes after overexpression and interference with circINSR. The results showed that circINSR promoted the expression of anti-apoptotic gene *Bcl-2* and inhibited the expression of pro-apoptotic genes *BAX* and *Caspase*9 (Fig. 6A, B). At the same time, Western Blots got the same trend (Fig. 6C). In contrast, real-time qPCR results showed that overexpression of miR-15/16 inhibited *Bcl-2* gene expression and promoted *BAX* and *caspase*9 expression. The co-transfection of circINSR inhibited the apoptosis of preadipocytes (Fig. 6D). To further verify that circINSR can inhibit cell apoptosis by adsorbing miR-15/16 family, we used Annexin V-PE/7-AAD staining combined with flow cytometry to analyze the effects of co-transfection of miR-15/16 and circINSR on cell apoptosis. The results showed that miR-15/16 promoted cell apoptosis, and co-transfection with circINSR rescued this anti-apoptotic effect (Fig. 6E, F).

3.6 CircINSR inhibits preadipocytes differentiation.

According to the above results, circINSR could promote the proliferation of myoblasts and preadipocytes, and inhibit cell apoptosis. We further studied the function of circINSR on the differentiation of preadipocytes. The results showed that overexpression of circINSR could inhibit the expression of adipogenic related genes *PPARγ*, *C/EBPα*, and *FABP4* (Fig. 7A, B). In contrast, interference with circINSR promoted the expression of these genes (Fig. 7C, D). BODIPY staining can directly observe the formation of lipid droplets in adipocytes through green fluorescence. Given that the circINSR overexpression vector carries GFP fluorescence, we only analyzed the BODIPY staining after interference with circINSR. 8 days after induction, the cells were conducted by BODIPY staining. The results showed that si-circINSR significantly increased the intensity of green fluorescence in preadipocytes (Fig. 7E). In addition, the staining results of Oil Red O also showed that overexpression of circINSR inhibited the lipogenesis of precursor fat, and the accumulation of lipid droplets increased after interference with circINSR (Fig. 7F).

In order to further analyze whether the effect of circINSR on adipogenesis is related to miR-15/16, we found two reported target genes of miR-15/16, *FOXO1* and *EPT1* (*SELENOI*) (Fig. 8A). Real-time qPCR results showed that the expressions of *FOXO1* and *EPT1* were significantly reduced after miR-15/16 overexpression, and co-transfection with circINSR rescued this inhibition (Fig. 8B). In addition, miR-15/16 promoted the expression of adipogenic genes, while circINSR inhibited the expression of adipogenic genes (Fig. 8C). The results of Oil Red O staining showed that miR-15/16 promoted lipid accumulation in preadipocytes, while co-transfection with circINSR inhibited adipogenesis (Fig. 8D, E).

4. Discussion

Myoblasts and intramuscular adipocytes are derived from mesenchymal stem cells (MSCs). Under complex signal regulation, some MSCs differentiate into myogenic and non-myogenic cell lines. Myogenic cells enter the process of muscle development, while non-myogenic cells enter the process of adipogenesis or fibroblast development(20, 21). At about 180 days of gestation in bovine fetuses, the IMF

begins to appear. But before that, the adipogenic progenitor cells have already begun to differentiate into preadipocytes(22). Therefore, we can separate myoblasts and intramuscular preadipocytes by using enzyme digestion combined with differential adhesion screening.

In this study, the isolated myoblasts were of high purity, and thick myotubes were labeled with anti-MyHC fluorescent antibody after 4 days of differentiation. However, the isolated preadipocytes contained MSCs, fibroblasts and adipogenic progenitor cells, which affected the cell purity. Combining cell surface marker proteins (such as CD140a) and flow cytometry sorting might be able to obtain higher purity preadipocytes(23). Nevertheless, the preadipocytes were also successfully induced to differentiate, and lipid droplets were identified using Oil Red O and BODIPY staining.

The development of muscle and fat is regulated by a complex signal network involving coding genes and non-coding RNAs. In this study, the expression of *PPARγ* and *C/EBPa* in differentiated preadipocytes increased significantly. And after 4 days of myogenic differentiation, *MyOD* and *MyHC* expression increased significantly. These coding genes played an important role in the differentiation of muscle and fat. In addition, more and more reports proved that non-coding RNAs are also involved in the regulation of muscle and fat development.

The circINSR is highly homologous to human has_circ_0048966, formed by the head-to-tail splicing of *INSR* second exon (552 bp), and is mainly expressed in the cytoplasm. In previous research, circINSR regulates cells proliferation and apoptosis through miR-34a-modulated *Bcl-2* and *CyclinE2* expression(17). In this study, we found that circINSR could also sponge the miR-15/16 family. The real-time qPCR results showed that overexpression of circINSR in myoblasts and preadipocytes could significantly inhibit the expression of miR-15/16 family. Dual fluorescence analysis and Ago2-RIP results also illustrated this adsorption relationship. Therefore, according to the molecular mechanism of sponging miRNAs, circRNAs should have the same targeting ability in view of the same seed sequence of miRNAs family.

In animals, single-stranded miRNAs binds specific mRNAs through sequences that are imperfectly complementary to the target mRNAs, mainly to the 3'-UTR(24). Existing studies have reported the regulatory mechanism of *Bcl-2* and *CyclinD1* in cancer cells consisting of posttranscriptional down-regulation by miR-15 and miR-16(25-27). In this study, we verified the interaction of miR-15/16 with *Bcl-2* and *CyclinD1*. Overexpression of miR-15/16 in myoblasts and preadipocytes promoted cell proliferation and inhibited apoptosis. Much more, the effect of miR-15/16 was counteracted when circINSR was co-transfected. The results indicated that during the embryonic stage, circINSR could promote muscle development and increase the number of intramuscular preadipocytes.

The number of intramuscular preadipocytes is the guarantee for the marbling during fattening. However, the premature maturation of the IMF may lead to fetal muscle insufficiency and wasted of nutrition during pregnancy. For example, the early muscle tissue of Duchenne muscular dystrophy is manifested as muscle fiber regeneration and mild lipid droplets, and the late muscle fibers are gradually replaced by fat and connective tissue, which seriously affects muscle function. Studies have pointed out that miR-

15/16 promotes adipogenesis by targeting *FOXO*1 and *EPT*1 genes(28, 29). In our results, the overexpression of circINSR in preadipocytes inhibited the expression of key genes for adipogenic differentiation and reduced lipid droplet formation. And the function of inhibiting adipogenesis is achieved by sponging miR-15/16. Therefore, the function of circINSR to inhibit adipogenesis in the fetal period can maintain the normal muscle function while ensuring the number of intramuscular preadipocytes.

5. Conclusions

In conclusion, our results reveal that circINSR negatively regulates miR-15/16 family expression. CircINSR promotes the proliferation of myoblasts and preadipocytes and inhibits apoptosis. And inhibit the differentiation of intramuscular preadipocytes to ensure the normal development of embryonic muscle. These results provide potential molecular targets for improving beef production and molecular breeding.

6. Abbreviations

IMF: intramuscular fat; AGO2: Argonaute2 protein; *PPARγ*: peroxisome proliferative activated receptor; *C/EBPα*: CCAAT/enhancer binding protein; *MRFs*: myogenic regulatory factors; *MEF*2: myocyte enhancer factor; MSCs: mesoderm mesenchymal stem cells; INSR: insulin receptor; EdU: 5-ethynyl-20-deoxyuridine; CCK-8: cell counting kit-8; circRNAs: circular RNAs; ceRNA: competitive endogenous RNA; MyHC: myosin heavy chain isoforms; NC: negative control; 7-AAD: 7-aminoactinomycin; BODIPY 493/503: 4,4-difluoro-1,3,5,7,8-pentamethyl-4-bora-3a,4a-diaza-s-indacene; RIP: RNA binding protein immunoprecipitation;

7. Declarations

Funding

This work was supported by the National Natural Science Foundation of China [Grant No. 31772574], Major project of collaborative innovation of industry, university, research and application in Yangling Demonstration Zone [2018CXY-05]. The funders had no role in study design, data collection and analysis, decision to publish, or preparation of the manuscript.

Availability of data and material

The datasets used and analyzed during the current study are available from the corresponding author on reasonable request.

Authors' contributions

H. Chen and X. M. Shen designed research; X. M. Shen, X. Y. Zhang, W. X. Ru and Y. Z. Huang performed experiments and analyzed data. X. M. Shen wrote the paper. C. Z. Lei and X. Y. Lan contributed new

analytic tools. H. Chen and J. Tang helped modify the language of this manuscript. The authors declare they have no competing financial interest and no conflicts of interest.

Ethics approval and consent to participate

All animal experiments and study protocols were approved by the Animal Care Commission of the College of Veterinary Medicine, Northwest A&F University.

Consent for publication

Not applicable.

Competing interests

The authors declare they have no competing financial interest and no conflicts of interest.

Acknowledgements

Not applicable.

8. References

1. Picard B, Berri C, Lefaucheur L, Molette C, Sayd T, Terlouw C. Skeletal muscle proteomics in livestock production. Brief Funct Genomics 9:259-278. Briefings in Functional Genomics. 2010;9(3):259-78.
2. Rehfeldt C, Fiedler I, Dietl G, Ender K. Myogenesis and postnatal skeletal muscle cell growth as influenced by selection. Livestock Production Science. 2000;66(2):177-88.
3. Sanchez-Gurmaches J, Guertin DA. Adipocyte lineages: Tracing back the origins of fat. Biochimica Et Biophysica Acta-Molecular Basis of Disease. 2014;1842(3):340-51.
4. Rajesh RV, Heo GN, Park MR, Nam JS, Kim NK, Yoon D, et al. Proteomic analysis of bovine omental, subcutaneous and intramuscular preadipocytes during in vitro adipogenic differentiation. Comparative Biochemistry & Physiology Part D Genomics & Proteomics. 2010;5(3):234-44.
5. Taga H, Bonnet M, Picard B, Zingaretti MC, Cassar-Malek I, Cinti S, et al. Adipocyte metabolism and cellularity are related to differences in adipose tissue maturity between Holstein and Charolais or Blond d'Aquitaine fetuses. J Anim Sci. 2011;89(3):711-21.
6. Tontonoz P, Hu E, Spiegelman BM. Stimulation of adipogenesis in fibroblasts by PPAR gamma 2, a lipid-activated transcription factor. Cell. 1994;79(7):1147-56.
7. Lin FT, Lane MD. CCAAT/enhancer binding protein alpha is sufficient to initiate the 3T3-L1 adipocyte differentiation program. Proceedings of the National Academy of Sciences of the United States of America. 1994;91(19):8757-61.
8. Soumillion A, Erkens JH, Lenstra JA, Rettenberger G, te Pas MF. Genetic variation in the porcine myogenin gene locus. Mammalian genome : official journal of the International Mammalian Genome Society. 1997;8(8):564-8.

9. Sassoon D, Lyons G, Wright WE, Lin V, Lassar A, Weintraub H, et al. Expression of two myogenic regulatory factors myogenin and MyoDI during mouse embryogenesis. Nature. 1989;341(6240):303-7.
10. Potthoff MJ, Olson EN. MEF2: a central regulator of diverse developmental programs. Development. 2007;134(23):4131-40.
11. McPherron AC, Lee SJ. Double muscling in cattle due to mutations in the myostatin gene. Proceedings of the National Academy of Sciences of the United States of America. 1997;94(23):12457-61.
12. Relaix F, Rocancourt D, Mansouri A, Buckingham M. A Pax3/Pax7-dependent population of skeletal muscle progenitor cells. Nature. 2005;435(7044):948-53.
13. Hansen TB, Jensen TI, Clausen BH, Bramsen JB, Finsen B, Damgaard CK, et al. Natural RNA circles function as efficient microRNA sponges. Nature. 2013;495(7441):384-8.
14. Meng S, Zhou H, Feng Z, Xu Z, Tang Y, Li P, et al. CircRNA: functions and properties of a novel potential biomarker for cancer. Mol Cancer. 2017;16(1):94.
15. Li H, Yang J, Wei X, Song C, Dong D, Huang Y, et al. CircFUT10 reduces proliferation and facilitates differentiation of myoblasts by sponging miR-133a. Journal of cellular physiology. 2018;233(6):4643-51.
16. Li H, Wei X, Yang J, Dong D, Hao D, Huang Y, et al. circFGFR4 promotes differentiation of myoblasts via binding miR-107 to relieve its inhibition of Wnt3a. Molecular Therapy-Nucleic Acids. 2018;11:272-83.
17. Shen XM, Zhang XY, Ru WX, Huang YZ, Lan XZ, Lei CZ, et al. circINSR Promotes Proliferation and Reduces Apoptosis of Embryonic Myoblasts by Sponging miR-34a. Molecular Therapy-Nucleic Acids. 2020;19:986-99.
18. Arcinas C, Tan W, Fang W, Desai TP, Teh DCS, Degirmenci U, et al. Adipose circular RNAs exhibit dynamic regulation in obesity and functional role in adipogenesis. Nature Metabolism. 2019;1(7):688-703.
19. Miyake M, Takahashi H, Kitagawa E, Watanabe H, Sakurada T, Aso H, et al. AMPK activation by AICAR inhibits myogenic differentiation and myostatin expression in cattle. Cell and tissue research. 2012;349(2):615-23.
20. Du M, Tong J, Zhao J, Underwood KR, Zhu M, Ford SP, et al. Fetal programming of skeletal muscle development in ruminant animals. J Anim Sci. 2010;88:E51-E60.
21. Stachecka J, Walczak A, Kociucka B, Ruszczycki B, Wilczyński G, Szczerbal I. Nuclear organization during in vitro differentiation of porcine mesenchymal stem cells (MSCs) into adipocytes. 2018;149(2):113-26.
22. Du M, Huang Y, Das AK, Yang Q, Duarte MS, Dodson MV, et al. MEAT SCIENCE AND MUSCLE BIOLOGY SYMPOSIUM: Manipulating mesenchymal progenitor cell differentiation to optimize performance and carcass value of beef cattle. J Anim Sci. 2013;91(3):1419-27.

23. Guan L, Hu X, Liu L, Xing Y, Zhou Z, Liang X, et al. bta-miR-23a involves in adipogenesis of progenitor cells derived from fetal bovine skeletal muscle. Sci Rep. 2017;7:43716.
24. Carthew RW, Sontheimer EJ. Origins and Mechanisms of miRNAs and siRNAs. Cell. 2009;136(4):642-55.
25. Pekarsky Y, Balatti V, Croce CM. BCL2 and miR-15/16: from gene discovery to treatment. Cell death and differentiation. 2018;25(1):21-6.
26. Cimmino A, Calin GA, Fabbri M, Iorio MV, Ferracin M, Shimizu M, et al. miR-15 and miR-16 induce apoptosis by targeting BCL2. Proceedings of the National Academy of Sciences. 2005;102(39):13944-9.
27. Pekarsky Y, Croce CM. Role of miR-15/16 in CLL. Cell Death & Differentiation. 2015;22(1):6-11.
28. Dong P, Mai Y, Zhang Z, Mi L, Wu G, Chu G, et al. MiR-15a/b promote adipogenesis in porcine pre-adipocyte via repressing FoxO1. Acta Biochim Biophys Sin (Shanghai). 2014;46(7):565-71.
29. Xu J, Zhang L, Shu G, Wang B. microRNA-16-5p promotes 3T3-L1 adipocyte differentiation through regulating EPT1. Biochem Biophys Res Commun. 2019;514(4):1251-6.

Figures

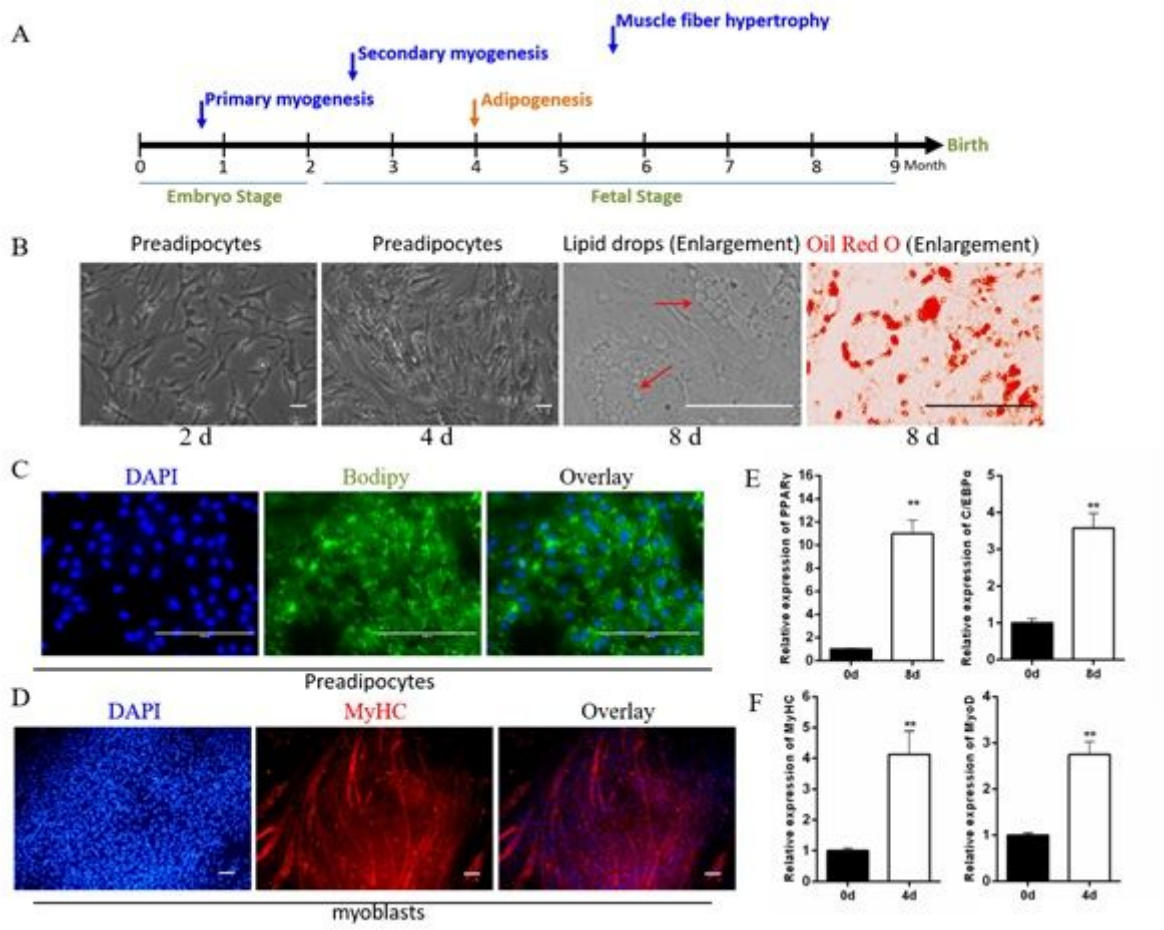

Figure 1

Identification of isolated myoblasts and intramuscular preadipocytes. (A) The growth pattern of muscle and fat during embryonic development of cattle. (B) The growth morphology of the isolated preadipocytes on day 2 and day 4, and the Oil Red O staining intracellular lipid droplets at 8 days of adipogenic differentiation. (C) BODIPY staining of preadipocytes at 8 days of adipogenic differentiation. (D) Anti-MyHC immunofluorescence staining of myoblasts at 4 days after myogenic differentiation. (E) The expression of adipogenic marker genes PPARγ and C/EBPα after differentiation of preadipocytes. (F) The expression of muscle differentiation marker genes MyHC and MyoD after differentiation of myoblasts. Data are presented as means ± SEM. *P < 0.05, **P < 0.01.

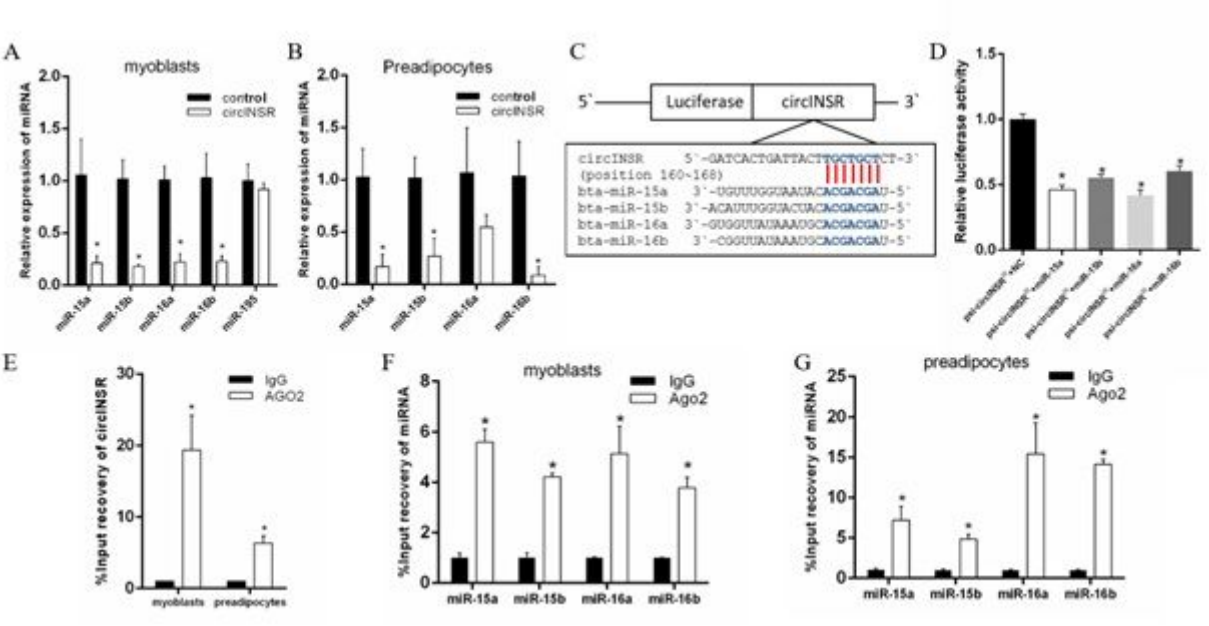

Figure 2

CircINSR could sponging miR-15/16 family in myoblasts and preadipocytes. (A) The changes of miR-15/16 family in myoblasts after overexpression of circINSR. (B) The changes of miR-15/16 family in preadipocytes after overexpression of circINSR. (C, D) Luciferase reporter activity of circINSR-WT in HEK-293T cells co-transfected with miR-15/16 mimics or mimics NC. (E) Ago2-RIP assay for the amount of circINSR in myoblasts and preadipocytes. (F) Ago2-RIP assay for the amount of miR-15/16 family in myoblasts. (G) Ago2-RIP assay for the amount of miR-15/16 family in preadipocytes. Data are presented as means ± SEM. *P < 0.05.

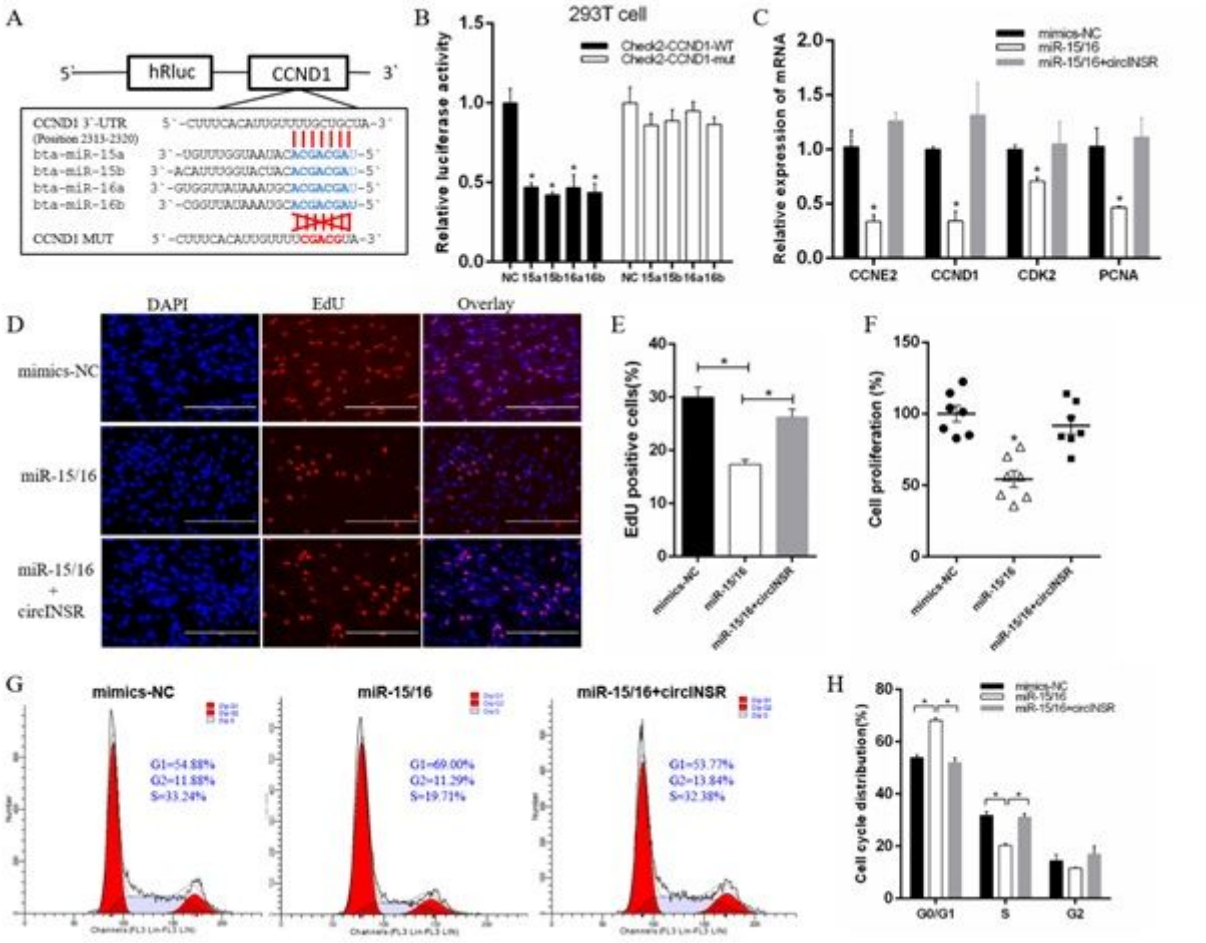

Figure 3

CircINSR promotes myoblasts proliferation by sponging the miR-15/16 family. (A) TargetScan predicted that CyclinD1 3'-UTRs had binding sites for miR-15/16. (B) The fluorescence activity changes after co-transfection with dual fluorescent reporter vectors and miR-15/16. (C) The expression of marker genes related to cell proliferation after co-transfection of circINSR and miR-15/16 in myoblasts. (D, E) EdU assay for myoblasts transfected with miR-15/16 mimics alone or co-transfected with circINSR. Scale bars, 200 μm. (F) CCK-8 assay for myoblasts transfected with miR-15/16 mimics alone or co-transfected with circINSR. n=6. (G, H) Cell cycle assay for myoblasts transfected with miR-15/16 mimics alone or co-transfected with circINSR. Data are presented as means ± SEM. *P < 0.05.

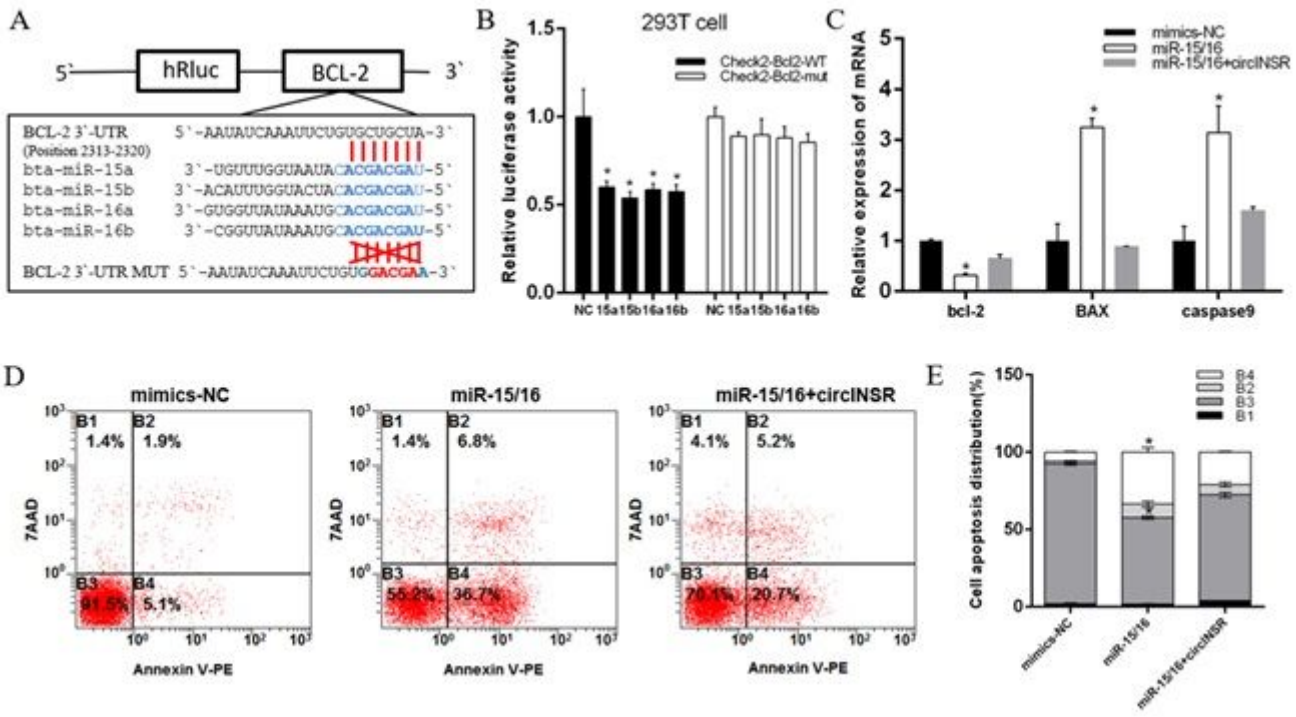

Figure 4

CircINSR inhibits the apoptosis of bovine primary myocytes by sponging the miR-15/16 family. (A) TargetScan predicted that Bcl-2 3'-UTRs had binding sites for miR-15/16. (B) The fluorescence activity changes after co-transfection with dual fluorescent reporter vectors and miR-15/16. (C) The expression of marker genes related to cell apoptosis after co-transfection of circINSR and miR-15/16 in myoblasts. (D, E) Cell apoptosis was determined by Annexin V/7-AAD dual staining followed by flow cytometry. n=3. Data are presented as means ± SEM. *P < 0.05.

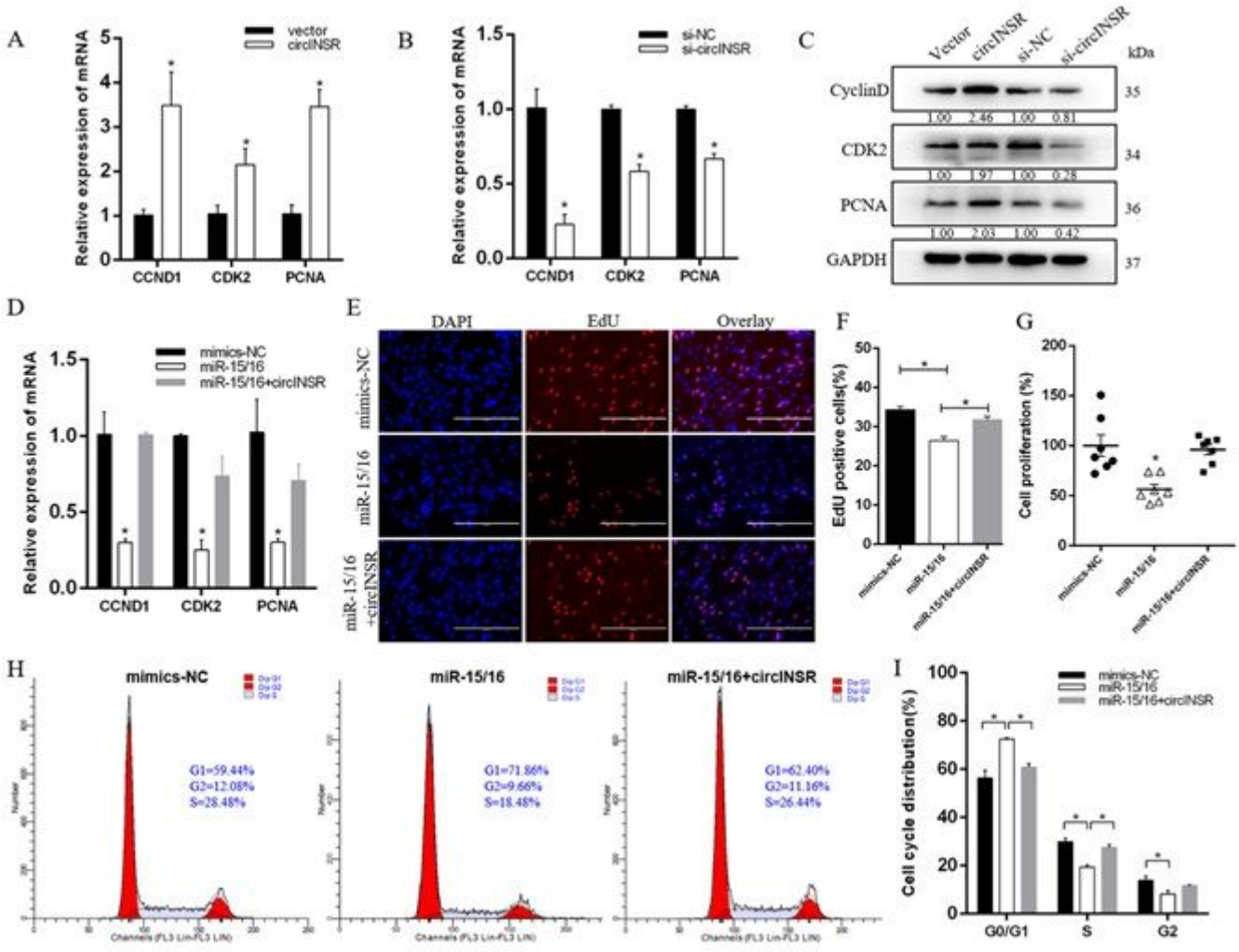

Figure 5

CircINSR promotes preadipocytes proliferation by sponging the miR-15/16 family. (A, B) In preadipocytes, the effect of overexpression and interference with circINSR on proliferation marker genes. (C) The expression of CCND1, CDK2, and PCNA was detected by Western Blots. (D) The expression of marker genes related to cell proliferation after co-transfection of circINSR and miR-15/16 in preadipocytes. (E, F) EdU assay for preadipocytes transfected with miR-15/16 mimics alone or co-transfected with circINSR. Scale bars, 200 μm. (G) CCK-8 assay for preadipocytes transfected with miR-15/16 mimics alone or co-transfected with circINSR. n=6. (H, I) Cell cycle assay for preadipocytes transfected with miR-15/16 mimics alone or co-transfected with circINSR. Data are presented as means ± SEM. *P < 0.05.

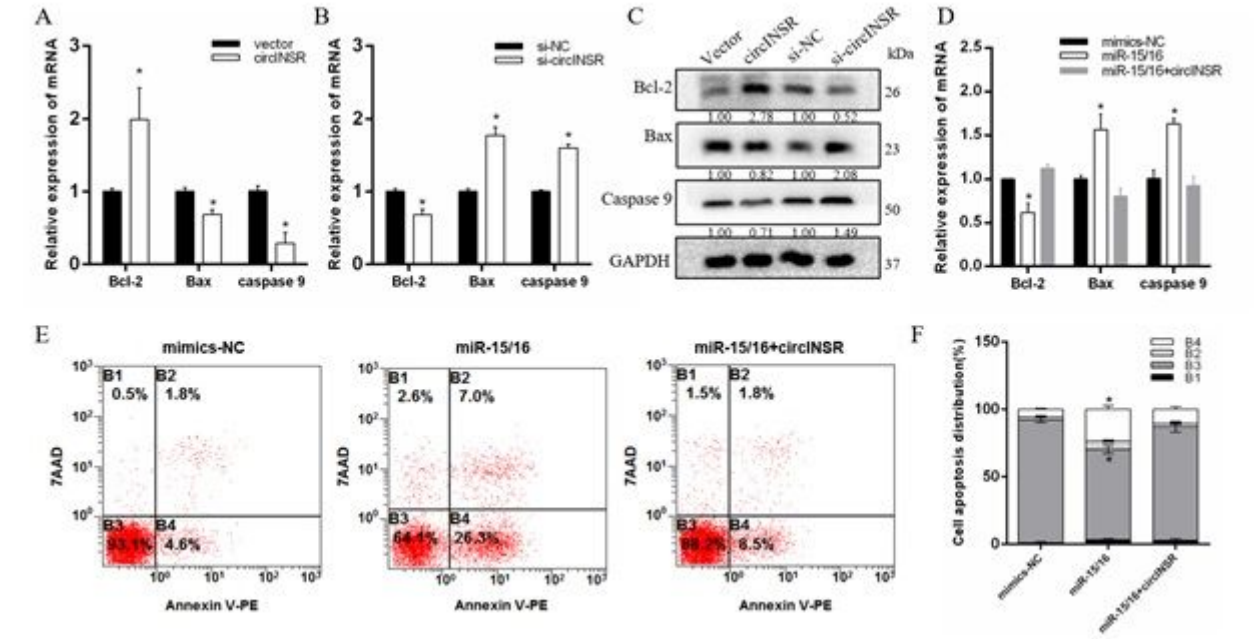

Figure 6

CircINSR inhibits preadipocytes apoptosis by sponging the miR-15/16 family. (A, B) The mRNA levels of cell apoptosis markers, including Bcl-2, Bax, and Caspase9 were detected by real-time qPCR in preadipocytes transfected with circINSR or siRNA. (C) The protein expression of Bcl-2, Bax, and Caspase9 was detected by Western Blots. (D) The expression of marker genes related to cell apoptosis after co-transfection of circINSR and miR-15/16 in preadipocytes. (E, F) Cell apoptosis was determined by Annexin V/7-AAD dual staining followed by flow cytometry. n=3. Data are presented as means ± SEM. *P < 0.05.

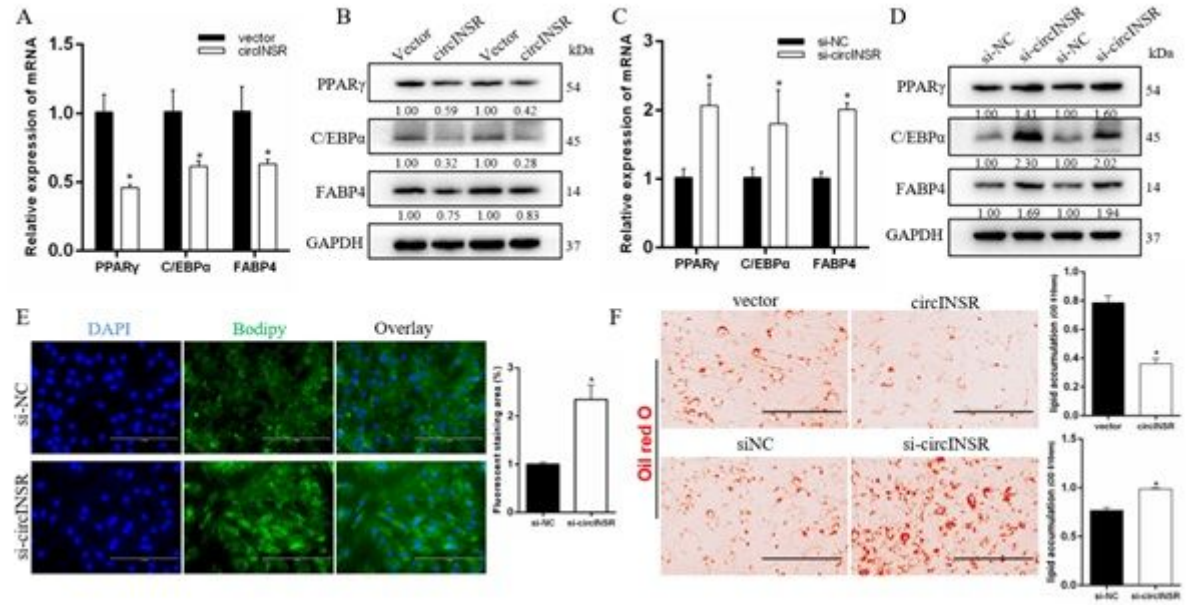

Figure 7

CircINSR inhibits adipogenic differentiation of preadipocytes. (A, B) The expression of adipogenic marker genes after overexpression of circINSR in preadipocytes was detected by real-time qPCR and Western Blots. (C, D) The expression of adipogenic marker genes after interference with circINSR in preadipocytes was detected by real-time qPCR and Western Blots. (E) Interference with circINSR in pre-adipocytes, BODIPY staining to analyze lipid droplet deposition. The fluorescence signal was analyzed by image J software. (F) Lipid droplets in preadipocytes were stained with Oil Red O. Lipid content measured by spectrophotometric analysis after dissolving in isopropanol. Data are presented as means ± SEM. *P < 0.05.

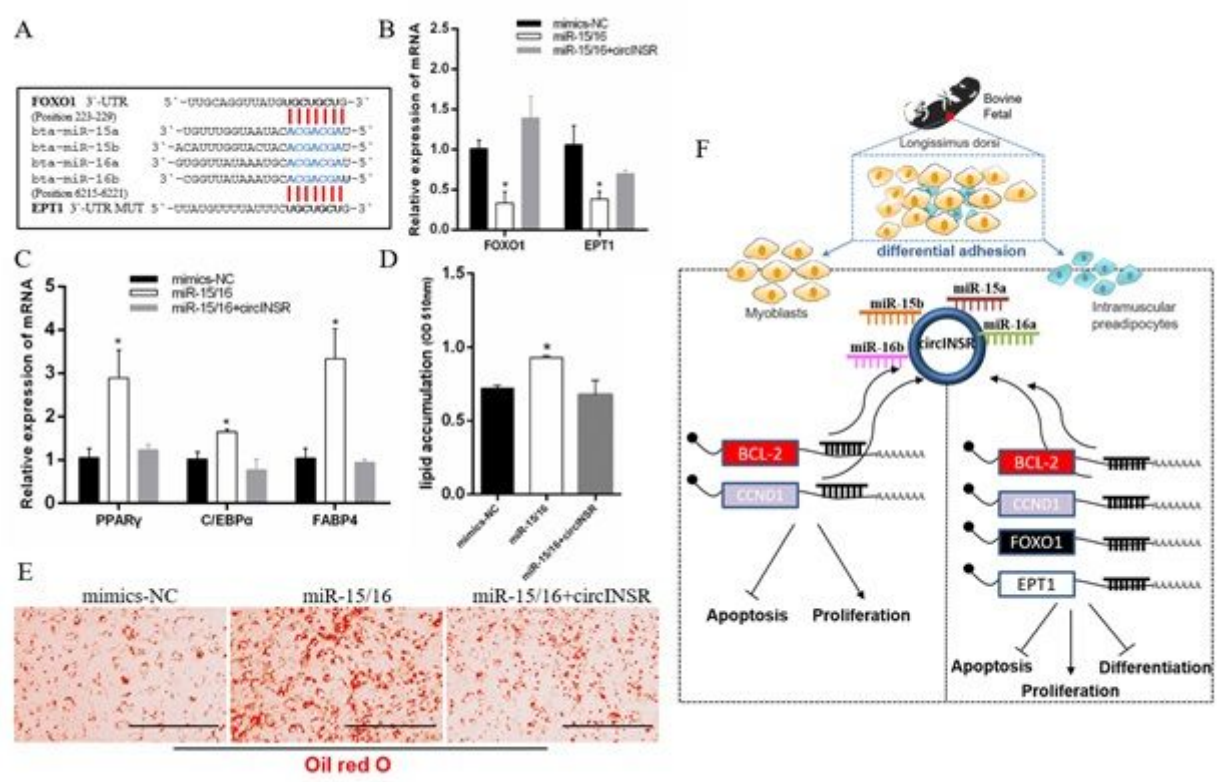

Figure 8

Adipogenic differentiation was regulated by circINSR through miR-15/16. (A) The reported target genes of the miR-15/16 family. (B) The effect of miR-15/16 or co-transfection with circINSR on target genes in preadipocytes. (C) The expression of adipogenic marker genes in preadipocytes was detected by real-time qPCR. (D, E) Lipid droplets in preadipocytes were stained with Oil Red O. Lipid content measured by spectrophotometric analysis after dissolving in isopropanol. Data are presented as means ± SEM. *P < 0.05. (F) Schematic diagram of circINSR regulating the proliferation, apoptosis and differentiation of myoblasts and preadipocytes.